

Unique 1- q and 3- q incommensurate phases in proustite: ^{75}As NQR line-shape and spin-lattice relaxation study

T. Apih, U. Mikac, J. Dolinšek, J. Seliger, and R. Blinc
J. Stefan Institute, Ljubljana, Slovenia

(Received 27 July 1999)

^{75}As NQR spectra and spin-lattice relaxation time T_1 have been measured between room temperature and 4.2 K in a proustite (Ag_3AsS_3) single crystal. In agreement with x-ray scattering data we find that the phase between $T_I=60$ K and $T_L=49$ K is triple- q (3- q) incommensurably modulated. Our results show unambiguously that we deal here with three independent noncoplanar incommensurate modulation wave vectors. Such a phase seems to be unique in a sense that other phases with three incommensurate modulation waves known so far (e.g., in charge-density-wave systems) are either a superposition of differently oriented 1- q modulated domains, or the three modulation waves are confined to a plane and are thus not independent. In addition the ^{75}As NQR line shape suggests that the phase just below T_I is a single- q (1- q) modulated stripe phase. This is confirmed by the variation of T_1 over the NQR line in the 1- q and 3- q phases. On further cooling further into the incommensurate phase the volume fraction of the 3- q phase gradually increases and the crystal becomes fully 3- q modulated about 2 K below T_I . The nonclassical critical exponents for the amplitude of the order parameter were determined to be $\beta_1=0.3\pm 0.02$ in the 1- q stripe phase and $\beta_3=0.4\pm 0.02$ in the 3- q phase. On approaching the lock-in transition temperature in the low-temperature part of the 3- q incommensurate phase the phases of the modulation waves become nonlinear functions of the corresponding spatial coordinates, resulting in sharp peaks superimposed on the broad bell-shape frequency distribution. A comparison between experimental and theoretical line shapes allowed for a quantitative determination of the temperature dependence of the soliton density.

I. INTRODUCTION

Structurally incommensurate systems are characterized by the modulation of some local atomic property, which varies in space in such a way that its periodicity is an irrational fraction of the periodicity of the host lattice.¹⁻⁴ As a result, translational periodicity along the modulation wave vector is lost in spite of the existence of perfect long-range order of the two subsystems. Phase transitions leading to an incommensurate phase with a single (1- q) modulation wave are described with a two-component order parameter³

$$Q_{\pm} = \rho \exp(\pm i\varphi), \quad (1)$$

where ρ stands for the amplitude and $\varphi = \mathbf{q} \cdot \mathbf{r} + \varphi_0$ for the phase. For this system (the most investigated example being Rb_2ZnCl_4) one usually expects a second-order phase transition from a paraelectric normal (N) phase to an incommensurate (IC) phase at a temperature T_I , and a lock-in transition to a ferroelectric commensurate (C) phase at a lower temperature T_C .

In the general case, however, incommensurate phases may be formed where not only one but several spatially periodic modulations with wave vectors \mathbf{q}_i are incommensurate with the characteristic wave vectors of the underlying lattice. For such a case phases of different symmetries may occur in the phase diagram. Let us consider a system with three (3- q) modulation waves, described by a six-component order parameter

$$Q_{\pm i} = \rho_i \exp(\pm i\varphi_i(\mathbf{x}_i)), \quad i=1,2,3. \quad (2)$$

This situation is realized in many charge-density-wave (CDW) systems, such as 2H-TaSe_2 ,⁵⁻⁷ as well as in structurally incommensurate quartz⁸ and berlinite (AlPO_4).⁹ For such a system two rather different structures may be realized below T_I .

(i) In the *stripe* or 1- q multidomain state the amplitude of a single modulation wave is different from zero in a given domain. Therefore, each domain is modulated in a single direction, but the direction of the modulation wave vector varies from one domain to another.

(ii) In an ‘‘all- q ’’ state, on the other hand, the amplitudes of all modulation waves are different from zero. In this case the crystal is modulated by a superposition of modulation waves with all q_i 's.

It is interesting to note that in every 3- q system known so far, both in CDW systems as well as in structurally incommensurate insulators such as quartz and AlPO_4 , the three modulation wave vectors lie in a plane, i.e., the number of modulation wave vectors is larger than the dimension of the space they span. This means that translational periodicity is retained in the direction perpendicular to the plane of the modulation waves. In this case the phases of the modulation waves are necessary correlated and the modulation waves are not independent. Such a situation occurs in both quartz^{8,10} and berlinite⁹ where the three modulation waves are coplanar, $\mathbf{q}_1 + \mathbf{q}_2 + \mathbf{q}_3 = 0$, and their relative phase is fixed, $\varphi_{01} + \varphi_{02} + \varphi_{03} = \varphi_{\Sigma} = 0, \pm\pi/2$ or π . Proustite (Ag_3AsS_3) seems to represent a unique exception, as x-ray measurements^{11,12} indicate that the incommensurate phase¹³ in the temperature range 49–60 K is modulated by three noncoplanar modulation waves. In such a system one can expect to observe a

number of phenomena, which were up till now predicted theoretically only.^{10,14} The soft mode should split into three gapless phason modes and three amplitude modes at the normal to incommensurate transition. In contrast to this, only two phason modes are gapless in a planar 3- q system, such as quartz,¹⁰ where the phase of the third modulation wave is well defined with respect to the others. Transition from a plane-wave regime, in which the phases of the modulation waves are linear functions of the space coordinates to a multisoliton regime, where they become steplike functions, has also not been observed for such a system as yet. In addition to soliton wall crossings (i.e., line defects), found in planar 3- q systems, there should be *triple* crossings (i.e., point defects) in a nonplanar 3- q system. As for other multi- q systems, there is a strong possibility of finding a transition between the “all- q ” phase and the multidomain 1- q stripe phase.^{10,14–17} Another point of interest is the study of critical exponents at the normal to incommensurate transition of a six-component order-parameter system. These should be different from the ones found in two-component order-parameter incommensurate systems that belong to the three-dimensional two-component (XY) model, with $\beta = 0.345$.¹⁸

In order to shed some additional light on some of the above phenomena, we performed a detailed ⁷⁵As NQR lineshape and spin-lattice relaxation study of a proustite single crystal²⁰ between room temperature and 4 K. An additional motivation to study such a phase was that it is very difficult to discriminate by x rays between a true 3- q phase and a 1- q multidomain stripe state. NMR and NQR, on the other hand, are *local* methods that measure the local distribution of displacements, which drastically differs for the stripe and “all- q ” phases and should thus easily discriminate between these two cases.

The usefulness of NMR and NQR for the study of incommensurate systems is due to the fact that the resonance frequency varies in space in a way which reflects the spatial variation of the incommensurate modulation.^{3,4} In commensurate systems the number of magnetic resonance lines equals the (usually very small) number of physically nonequivalent nuclei per unit cell. In incommensurate systems, where the translational lattice periodicity is lost, there is in essence an infinite number of nonequivalent nuclei contributing to the magnetic resonance spectrum. The incommensurate spectra are thus characterized by a quasicontinuous distribution of NMR frequencies instead of a sharp line as in commensurate crystals. The characteristic features of an incommensurate spectrum were shown^{9,19,20} to depend on the number of modulation waves and the dimension of space they span. For a 1- q IC system with a two-component order parameter (as well as for 1- q multidomain “stripe” state of a six-component order-parameter IC system), one expects a characteristic frequency distribution with two edge singularities, whereas a bell-like distribution with no singularities is expected for a 3- q noncoplanar IC system.¹⁹

II. PROUSTITE STRUCTURE AND PHASE TRANSITIONS

The proustite structure belongs to a noncentrosymmetric trigonal space group $R3c(C_{2v}^6)$ with two formula units per primitive rhombohedral unit cell at room temperature.²¹ The covalently bonded AsS₃ pyramids occupy the C₃ sites at

eight corners of the rhombohedral unit cell and one in the center, while the Ag atoms reside on the C₁ sites in the voids, formed by the S atoms. The unit cell contains 12 positions for Ag⁺ ions, six of them being vacant at room temperature. The AsS₃ pyramids are ionically bound by S—Ag—S bonds which form helices in the direction of the trigonal c axis. This rather weak bonding leads to a high ionic conductivity and allows Ag⁺ ions to adopt a quasi-free state. The consecutive AsS₃ pyramids along the c axis undergo a small relative rotation, each pyramid being related to the one above or below by a glide plane σ_v^g .

On cooling below room temperature, proustite exhibits several phase transitions: a transition from the high-temperature normal (N) phase to an incommensurate (IC) phase at $T_I \approx 60$ K, a lock-in transition to a commensurate phase C₁ at $T_L \approx 49$ K,¹² and a transition to nonmodulated ferroelectric phase C₂ at $T_{C_2} \approx 24$ K. At high pressures the intermediate IC and C₁ phases are suppressed,²² so that proustite exhibits a direct N-C₂ transition. In addition to this, it has been suggested that a photoinduced phase transition occurs near 210 K,²² connected to a redistribution of Ag⁺ ions under the action of illumination. In contrast to this, a detailed Raman scattering²⁴ and a combined neutron and x-ray diffraction study²⁵ (both conducted in the dark) failed to reveal any anomalies in the temperature range 80–300 K.

X-ray studies^{11,12} have shown that the second-order phase transition from the normal to the incommensurate phase characterized by a star of six wave vectors

$$\begin{aligned} \mathbf{q}_{\pm 1} &= \pm \left[\frac{1}{3} - \delta_a, -\left(\frac{1}{3} - \delta_a\right), 0, \frac{1}{3} - \delta_c \right], \\ \mathbf{q}_{\pm 2} &= \pm \left[0, \frac{1}{3} - \delta_a, -\left(\frac{1}{3} - \delta_a\right), \frac{1}{3} - \delta_c \right], \\ \mathbf{q}_{\pm 3} &= \pm \left[-\left(\frac{1}{3} - \delta_a\right), 0, \frac{1}{3} - \delta_a, \frac{1}{3} - \delta_c \right], \end{aligned} \quad (3)$$

where the hexagonal setting of the rhombohedral cell is adopted. Just below T_I δ_a and δ_c have values of 0.0063 and 0.0125, respectively. Both δ_a and δ_c are temperature dependent and decrease with decreasing temperature. Hence, not just the period but, while remaining in the glide plane, also the direction of the modulation varies as a function of temperature.

Pokrovsky and Pryadko¹⁵ have described the IC phase in proustite in terms of the Landau theory. They used the order parameter $\eta_i(\mathbf{r})$ which represents the Fourier components of the displacements $\mathbf{u}(\mathbf{r})$ with respect to the commensurate directions $\mathbf{q}_1^c = \frac{1}{3}[1, \bar{1}, 0, 1]^*$, $\mathbf{q}_2^c = \frac{1}{3}[0, 1, \bar{1}, 1]^*$, and $\mathbf{q}_3^c = \frac{1}{3}[\bar{1}, 0, 1, 1]^*$:

$$\mathbf{u}(\mathbf{r}) = \sum_{i=1}^3 \eta_i(\mathbf{r}) \xi(\mathbf{q}_i^c) \exp(i\mathbf{q}_i^c \mathbf{r}) + \text{c.c.} \quad (4)$$

Just below T_I they find that within constant amplitude approximation $\eta_i(\mathbf{r}) = \rho_i \exp(-i\varphi_i(\mathbf{r}))$, the free energy is minimized if the phases of the modulation waves are linear functions of the coordinates,

$$\varphi_i = \mathbf{k}_i \cdot \mathbf{r}. \quad (5)$$

Depending on the signs of the coefficients in the Landau expansion,¹⁵ either the 3-*q* or 1-*q* stripe phase may be realized below T_I :

$$\begin{aligned} 3-q: \quad \rho_1 = \rho_2 = \rho_3 = \rho/\sqrt{3} \propto \sqrt{t} \quad \text{for } C_1 > 0, \\ 1-q: \quad \rho_2 = \rho_3 = 0, \quad \rho_1 \propto \sqrt{t} \quad \text{for } C_1 < 0. \end{aligned} \quad (6)$$

Here t stands for the normalized temperature, $t = (T_I - T)/T_I$. If the sixth-order invariants²⁰ are included in the Landau expansion, both a 1-*q* stripe and 3-*q* phase may be stable below T_I . Depending on the size of the coefficients, either $N \rightarrow (3-q) \rightarrow C_1$, $N \rightarrow (1-q) \rightarrow C_1$, $N \rightarrow (1-q) \rightarrow (3-q) \rightarrow C_1$, or $N \rightarrow (3-q) \rightarrow (1-q) \rightarrow C_1$ phase sequences may be realized.²⁰

X-ray measurements^{11,12} did not reveal any structural change in the temperature region of the incommensurate phase 49–60 K. However, due to the low-temperature resolution of this measurements and due to the difficulties in discriminating between a true 3-*q* IC phase and a multidomain 1-*q* stripe phase by x rays, one cannot exclude the possibility of finding a 1-*q* stripe phase in a narrow temperature range either between the N and 3-*q* phase or between the 3-*q* and C_1 phase.

According to x-ray measurements^{11,12} the incommensurate parameters δ_a and δ_c vanish on cooling below the lock-in transition temperature $T_L = 49$ K (first order according to Ref. 11, second order according to Ref. 12) to a commensurably modulated phase C_1 . The C_1 unit cell has the volume 27 times that of the normal N phase but retains the same space group $R3c$, with the new crystallographic axes rotated by 180° with respect to N phase.

On cooling below $T_{C_2} = 24$ K proustite exhibits a strongly first-order phase transition to a ferroelectric phase C_2 where the structure is monoclinic with a space group Cc .²⁶ As S_3 pyramids are considerably distorted in the C_2 phase, the three As-S bond lengths differing by nearly 10%.²⁶ In addition to pyroelectric polarization along the c axis, a spontaneous component of polarization appears in the basal plane. In the ferroelectric phase the modulation of the normal phase disappears and the structure can be treated as a result of a new distortion of the N phase.¹⁵

III. EXPERIMENTAL

Zeeman perturbed ^{75}As ($I = \frac{3}{2}$) nuclear quadrupole resonance measurements of an optically pure proustite single crystal have been made at room temperature. In the high-temperature paraelectric phase all As nuclei in the unit cell lie on axially symmetric sites with $\eta = 0$. The quadrupole coupling constant varies from $e^2qQ/h = 132.44$ MHz at room temperature to 134.6 MHz at 62 K.

The phase transition to the incommensurate phase has been studied by zero-field ^{75}As NQR. Taking into account the photosensitivity of proustite, it is important that all measurements were performed in the dark in a helium flow cryostat. The width of the NQR spectrum changes from 10 kHz in the normal phase to 1.1 MHz in the incommensurate phase just above the phase transition to the commensurate phase. The broad line was measured by a ‘‘point-by-point’’ fre-

quency scanning method with an automatic tuning of the resonant circuit at each frequency. At each frequency ν_j , the spectral intensity $f(\nu_j)$ was obtained by integrating the Fourier transform of one half of the spin echo $S(\nu_j, t)$ following a $\pi/2$ - π pulse sequence. The frequency distribution $f(\nu)$ was thus obtained at a discrete set of resonance frequencies ν_j as

$$f(\nu_j) = \int_{-\Delta\nu/2}^{+\Delta\nu/2} \left(\int_0^\infty S(\nu_j, t) e^{i2\pi\nu t} dt \right) d\nu. \quad (7)$$

The typical frequency step $\Delta\nu = \nu_{j+1} - \nu_j$ was 5–10 kHz. Depending on the width of the resonance line, line-shape measurements took from a few minutes up to several hours. During the measurements the temperature gradient over the sample and the temperature stability were better than 0.05 K. At each change of the temperature (typically 0.1 K in the incommensurate phase) the sample was allowed to stabilize for an hour before performing the measurement.

The ^{75}As spin-lattice relaxation time was measured on Fourier-transformed NQR spectra, obtained by an ‘‘inversion-recovery’’ pulse sequence in the high-temperature normal phase and in the two low-temperature commensurate phases, where the resonance lines are narrow. In incommensurate phase, where inversion was not possible due to large linewidth, the ‘‘saturation-recovery’’ technique was used.

IV. ^{75}As NQR IN THE 1-*q* AND 3-*q* INCOMMENSURATE PHASES

It is well known^{4,19,27,28} that NQR (and quadrupole perturbed NMR) spectra of incommensurably modulated structures exhibit a characteristic inhomogeneous frequency distribution $f(\nu)$ that reflects the spatial variation of the NQR frequency. Instead of a few physically nonequivalent nuclear sites per unit cell as in translationally periodic crystals, we find in incommensurate systems, where the translational symmetry is lost, an essentially infinite number of non-equivalent nuclear sites resulting in a quasicontinuous frequency distribution.

The general formalism of calculating NMR and NQR line shapes by expanding electric field gradient (EFG) tensor in powers of the displacements of nuclei lying on the IC modulation wave was reported several times.^{4,19,27,28} In the case of ^{75}As ($I = \frac{3}{2}$) NQR the relation between the frequency shift and EFG tensor elements is particularly simple:

$$\nu = \frac{eQ}{2h} V_{zz}, \quad (8)$$

where $V_{zz} = V_{Nzz} + \delta V_{zz}$, V_{Nzz} is the principal eigenvalue of the EFG tensor in the high-temperature normal phase and δV_{zz} is a (small) space-dependent change due to the modulation wave(s). Applying the Taylor expansion of the EFG tensor components (in our case just V_{zz}) over the nuclear displacements in one dimensionally modulated (1-*q*) IC systems one gets^{4,19,27,28}

$$\begin{aligned} V = V_N + V_0 + V_1 \cos(\varphi(x) + \varphi_{10}) + V_2 \cos(2\varphi(x) + \varphi_{20}) \\ + \dots \end{aligned} \quad (9)$$

In the constant amplitude approximation, the coefficients V_i are constants. In the general case they are weakly x dependent. Using Eq. (8), we get a similar expression for the NQR frequency

$$\nu = \nu_N + \nu_0 + \nu_1 \cos(\varphi(x) + \varphi_{10}) + \nu_2 \cos(2\varphi(x) + \varphi_{20}) + \dots \quad (10)$$

The coefficient ν_1 is proportional to the amplitude of the order parameter, $\nu_1 \propto \rho \propto (T_I - T)^\beta$, while $\nu_2 \propto (T_I - T)^{\bar{\beta}}$. Most of 1- q IC systems belong to the three dimensional (3D) XY universality class where the critical exponents are $\beta = 0.35$ and $\bar{\beta} = 2 - \alpha - \phi = 0.84 \neq 2\beta$,^{18,29,30} but exceptions with the classic Landau exponents $\beta = 0.5$ and $\bar{\beta} = 2\beta = 1$ are also well known.³¹

The frequency distribution that determines the NQR line shape can be now evaluated by

$$f_{1-q}(\nu) = \int dx \delta[\nu - \nu(\varphi(x))]. \quad (11)$$

In NMR in incommensurate systems it is often the case that one is able to choose such an orientation of the sample with respect to the external magnetic field, that either the linear ($\nu_1 \neq 0$) or quadratic ($\nu_2 \neq 0$) term prevails in Eq. (10). Then the line shape is easily evaluated in the plane-wave regime where the phase of the modulation wave is a linear function of the spatial coordinate, $\varphi(x) = qx$. For the linear case ($\nu_1 \neq 0, \nu_2 = 0$) one gets^{3,4}

$$f_{1-q}(\nu) = \frac{\text{const}}{\sqrt{\nu_1^2 - (\nu - \nu_N)^2}}. \quad (12)$$

In this and also in the pure quadratic case, the IC spectrum is symmetric and limited by two edge singularities. A typical 1- q line shape for the linear case is shown in Fig. 1(a). If both linear and quadratic terms have to be taken into account in Eq. (10), a third and a fourth singularity may appear in the spectrum.^{3,27} This is often the case in NQR where the resonance frequency is independent of the crystal orientation and one is not able to control the parameters ν_i in Eq. (10) by varying an external parameter. In this general case the spectrum becomes asymmetric and its shape and number of singularities strongly depend on the ratio of the linear and the quadratic term and the relative phase shift between them.

Now we turn to the 3- q case, where the structure is simultaneously modulated by three modulation waves. The 3- q equivalent of Eq. (10) in the linear case is¹⁹

$$\nu(\varphi_1, \varphi_2, \varphi_3) = \nu_0 + \sum_{i=1}^3 \nu_i \cos \varphi_i, \quad (13)$$

where the ν_i are proportional to the amplitude of i th modulation wave. In the plane-wave limit we have

$$\varphi_i = \mathbf{q}_i \cdot \mathbf{r} + \varphi_{0i}. \quad (14)$$

Here the modulation wave vectors \mathbf{q}_i are incommensurate to the underlying lattice. The phases φ_i take on any value from the interval $[-\infty, +\infty]$ with equal probability. Instead of a

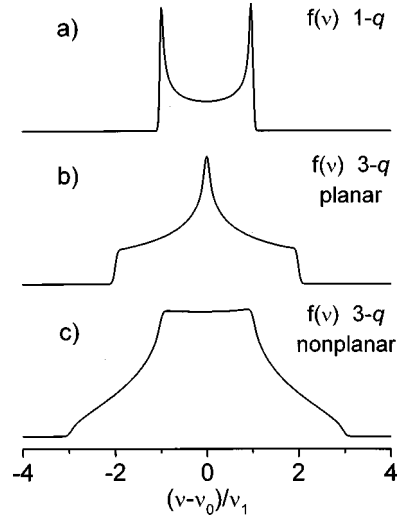


FIG. 1. Theoretical NQR line shapes in the plane-wave limit of (a) 1- q and (b), (c) 3- q incommensurate systems for a linear coupling between the NQR frequency shift and the displacement. In the 3- q planar case (b), where the modulation waves are confined to a plane, the line shape is similar to that of a 2- q IC system.^{19,9} In this case the position of the central singularity depends on the relative phases of the three modulation waves. The line shape is independent of the initial phases of the modulation waves in the nonplanar 3- q case (c).

single sharp NMR line in the high-temperature phase we find a characteristic frequency distribution in the incommensurate phase:

$$f_{3-q}(\nu) = \int dx_1 dx_2 dx_3 \delta[\nu - \nu(\varphi_1(\mathbf{r}), \varphi_2(\mathbf{r}), \varphi_3(\mathbf{r}))]. \quad (15)$$

Here the integration $\int dx_1 dx_2 dx_3$ must account for the possible correlation of the phases.^{9,19} When the modulation waves are independent, the frequency distribution $f(\nu)$ is given by a double convolution

$$f_{3-q}(\nu) = \int_{-\infty}^{+\infty} \int_{-\infty}^{+\infty} d\nu'_1 d\nu'_2 f_1(\nu'_1) f_2(\nu'_2) f_3(\nu - \nu'_1 - \nu'_2) \quad (16)$$

of frequency distributions $f_i(\nu')$ for single- q modulations:

$$f_i(\nu') = \int_{-\infty}^{+\infty} d\varphi_i \delta[\nu' - \nu(\varphi_i)] = \frac{\text{const}}{\sqrt{\nu_i^2 - \nu'^2}}. \quad (17)$$

A typical bell-like 3- q line shape for the linear case with $\nu = \nu_1 = \nu_2 = \nu_3$ is shown in Fig. 1(c). In contrast to 1- q IC line shape, there are no edge singularities in the 3- q IC line shape, but the derivative of the line has four van-Hove-like singular points.¹⁹ It is interesting to note that the 3- q IC line shape completely changes, if the three modulation waves are correlated. Such is the case in quartz^{8,10} and berlinite⁹ where the three modulation waves are coplanar, $\mathbf{q}_1 + \mathbf{q}_2 + \mathbf{q}_3 = 0$, and their relative phase is fixed. As shown in Refs. 9 and 19, in such a case the line shape is similar to that of a 2- q IC system with a logarithmic singularity at a position which depends on the relative phase.

While the static properties of the incommensurate modulation waves are reflected in the NQR spectra, the dynamic properties are expected to show up in the nuclear spin-lattice relaxation time T_1 .^{3,4,33} In translationally periodic crystals undergoing structural phase transitions the main contribution to the spin-lattice relaxation is usually made by the low-frequency soft optic modes. The contribution of long-wavelength acoustic modes is negligible as the relative displacements of the neighboring atoms are too small. Since the energy of an IC system is in the continuum limit independent of the initial phases of the IC modulation waves, this system has in addition to acoustic phonons n new independent modes, whose frequencies vanish for a particular \mathbf{q} value. These modes represent Goldstone excitations known as phasons. In the case of n -correlated modulation waves as it is the case in planar 3- q IC systems ($n=3$, $D=2$), such as quartz and berlinite, the number of gapless phasons is smaller than n . The number of thermally excited phasons is of the order of the acoustic phonons and the relative displacements are not small for the critical wave vector. Spin-lattice relaxation should be thus in incommensurate phases determined mainly by phasons.

For a system with n modulation waves linearly and locally related to the frequency shift one can write the spin-lattice relaxation rate as¹⁹

$$\frac{1}{T_1}(\varphi_1, \dots, \varphi_n) \propto \sum_{i=1}^n (\cos^2 \varphi_i J_{A_i} + \sin^2 \varphi_i J_{\phi_i}), \quad (18)$$

where the J_{A_i} and J_{ϕ_i} are the local spectral densities^{3,4,33} of the amplitudon and phason fluctuation modes. For 1- q IC systems ($n=1$), one finds in the linear case a simple relation between the effective spin-lattice relaxation rate T_1^{-1} and the NQR frequency shift.^{3,33} Here J_A determines T_1^{-1} at the edge singularities and J_ϕ determines T_1^{-1} in the middle of the inhomogeneously broadened NQR spectrum. The situation is more complicated for the case of a multi- q IC system. Here, at any given frequency, one does not have a single relaxation rate but a *distribution* of spin-lattice relaxation rates

$$F\left(\frac{1}{T_1}, \nu\right) = \int \cdots \int d\varphi_1 \dots d\varphi_n \delta(\nu - \nu(\varphi_1, \dots, \varphi_n)) \times \delta\left(\frac{1}{T_1} - \frac{1}{T_1}(\varphi_1, \dots, \varphi_n)\right), \quad (19)$$

and a nonexponential decay of magnetization is expected. In principle, one could use the inverse Laplace transform of the magnetization-decay curve to determine the T_1^{-1} distribution, from which the spectral densities J_{A_i} and J_{ϕ_i} could be inferred. However, in view of the complex shape of the T_1^{-1} distribution, calculated in the linear local approximation,¹⁹ one can immediately realize the complexity of such a task. In addition, if nonlocal contributions are expected, they will further complicate the T_1^{-1} distribution.^{27,33}

V. RESULTS AND DISCUSSION

A. Temperature dependence of NQR frequencies

The temperature dependence of the ^{75}As quadrupole resonance frequencies ν_Q and the spin-lattice relaxation time T_1

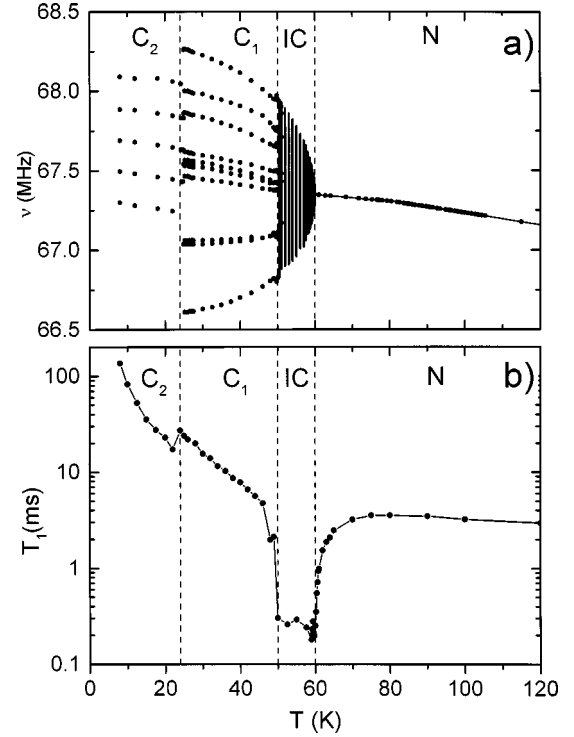


FIG. 2. Temperature dependence of the ^{75}As NQR frequencies ν_Q (a) and the average spin-lattice relaxation time T_1 (b) in proustite between 8 and 120 K. There is a single resonance line in the high-temperature N phase, an inhomogeneously broadened line (indicated by the vertical lines) in the incommensurate phase, ten resonance lines in the C_1 phase, and five lines in the C_2 phase. Note the critical decrease of T_1 at the N-IC transition and anomalous short temperature-independent phason-induced T_1 in the IC phase.

of proustite are shown in Fig. 2(a). At room temperature a single resonance line with a half-height full-width of 5 kHz is observed at $\nu_Q = 66.22$ MHz. On cooling the NQR frequency continuously increases to 67.3 MHz just above the transition to the incommensurate phase at $T_I = 60$ K. There is a slight, but still well observable change of ν_Q versus T slope at about 75 K. The linewidth does not change between room temperature and 60.2 K just above T_I (Fig. 3).

Below $T_I = 60$ K an inhomogeneous broadening of the resonance line is observed in the incommensurate phase. The linewidth at half height changes from 5 kHz just above T_I to about 1.1 MHz in the lower part of the incommensurate phase. On cooling a set of sharp lines appears on the broad incommensurate background about 2 K above T_L . The multiplet of sharp lines increases in intensity with decreasing temperature and completely replaces the broad background at the transition to the commensurate phase C_1 .

In the C_1 phase one observes 10 narrow lines of different intensity. At 28 K (Fig. 3) we have three lines of low intensity, six lines of medium intensity, and a single line of high intensity. The temperature dependence of the positions of this ten lines is shown in Fig. 2.

At the transition temperature to the low-temperature commensurate phase C_2 , $T_{C_2} = 24$ K, the asymmetric multiplet of ten lines is discontinuously replaced by a symmetric multiplet of five lines (Fig. 3), which persists down to the lowest studied temperature (8 K). A similar behavior of the ^{75}As NQR lines at the C_1 to C_2 transition was observed earlier,^{14,22}

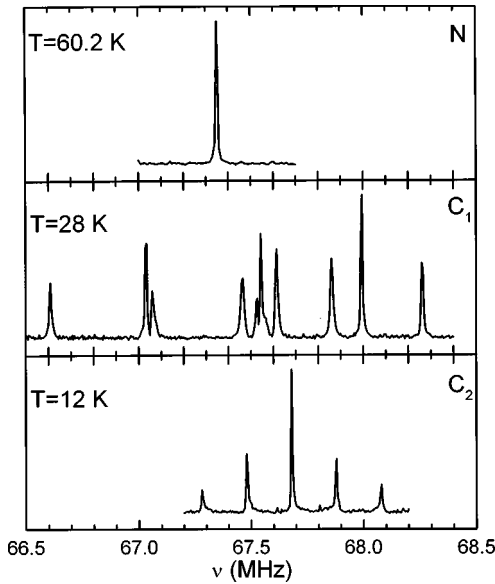


FIG. 3. ^{75}As NQR spectra in the three commensurate phases N (just above the N-IC transition), C_1 , and C_2 in a proustite single crystal.

but due to the lower sensitivity out of five only the most intense central line was observed.

B. Temperature dependence of T_1

The ^{75}As spin-lattice relaxation time T_1 [Fig. 2(b)], which amounts 1.5 ms at room temperature, increases monotonically and reaches a maximum value of 3.6 ms close to 75 K. There was no observable anomaly in the temperature dependence of either T_1 , resonance frequency ν_Q , or the linewidth $\Delta\nu$, which would indicate the (photoinduced) phase transition reported at 210 K.²³ Our experiments were performed in the dark and no attempt was made to check for the possible effect of the illumination on the parameters T_1 , ν_Q , and $\Delta\nu$. Below 75 K T_1 starts to decrease and a cusplike dip is observed in the vicinity of $T_I=60$ K, which is characteristic of a displacive structural transition with soft mode condensation.

The phason-induced average T_1 is anomalously short (~ 0.2 ms) and temperature independent in the incommensurate phase. The transition to C_1 phase is marked by a discontinuous increase of T_1 for an order of magnitude to $T_1=2$ ms just below T_{C_1} . In the C_1 phase $\ln(T_1)$ seems to increase linearly with decreasing temperature [Fig. 2(b)].

At $T_{C_2}=25$ K there is a discontinuous decrease from $T_1=27$ ms just above T_{C_1} to $T_1=17$ ms just below. On cooling, T_1 further increases to reach 135 ms at 8 K.

C. Line-shape analysis in the high-temperature part of the IC phase

As shown in Figs. 2 and 4, the narrow ^{75}As quadrupole resonance line of the high temperature N phase becomes inhomogeneously broadened below $T_I=60$ K, indicating the transition to an incommensurate phase. The broad line shape with two edge singularities, observed less than 1 K below T_I , is typical for a one dimensionally modulated (1- q) IC

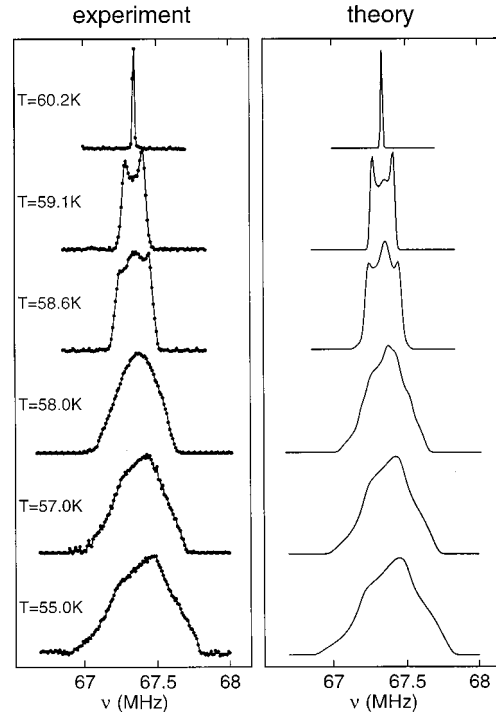


FIG. 4. Experimental and theoretical ^{75}As NQR line shapes in the high-temperature (plane-wave) part of the incommensurate phase in proustite. The theoretical spectra are calculated using formulas (26), (27), and (28). The temperature dependences of ν_1 , ν_2 , and R_{1-q} obtained from the fits are shown in Figs. 5 and 6.

system in the plane-wave limit. In the case of 3- q IC system with simultaneous modulations along \mathbf{q}_1 , \mathbf{q}_2 , and \mathbf{q}_3 , instead of the U-like line shape, a bell-like line shape with no edge singularities is expected (Fig. 1). On the other hand, the same line shape as in the 1- q case is expected in the multi-domain ‘‘stripe’’ phase, where in a given domain the structure is modulated along one of the modulation waves \mathbf{q}_1 , \mathbf{q}_2 , or \mathbf{q}_3 , while the amplitude of the other modulations is zero in this case. Since the modulation-induced shift of the resonance frequency does not depend on the direction of the modulation wave vector, the same expression (10) is valid for all of the 1- q domains:

$$\nu_{1-q} = \nu_N + \nu_0 + \nu_1 \cos(\varphi(x) + \varphi_{10}) + \nu_2 \cos(2\varphi(x) + \varphi_{20}) + \dots, \quad (20a)$$

and the line shape is given by the integral

$$f_{1-q}(\nu) = \int dx \delta[\nu - \nu_{1-q}(\varphi(x))]. \quad (20b)$$

Since the spectra are slightly asymmetric, it is clear that the coupling between the frequency and the order parameter is nonlocal and that both linear and quadratic terms of Eq. (20) must be used to describe the line shape.

On cooling further into the IC phase an asymmetric bell-like spectral component appears, which gradually replaces the 1- q spectrum. This component, which dominates the spectrum already 2 K below T_I , is typical¹⁹ of a 3- q modulated system with three independent nonplanar modulation waves. A similar bell-like ^{109}Ag NMR line shape was also observed in proustite at $T=55$ K.³² Note that NMR and

NQR can easily distinguish between the nonplanar and planar 3- q case, as completely different line shape with a central singularity is expected in the latter case.⁹ We have thus observed a transition from a stripe state, characterized by a superposition of 1- q modulated domains to a genuine 3- q state where the crystal is simultaneously modulated along three different directions. While this change of the structure was not observed before, it is not totally unexpected, as already the Pokrovsky free energy [Eq. (7)] predicts, that either a 1- q stripe state, a 3- q state, or a transition between the two is possible below T_I .^{15,20} The possibility of 1- q to 3- q transitions is also predicted by numerical simulations of molecular dynamics¹⁶ in hexagonal models. The transition between the two states with different symmetry is discontinuous and connected to metastable states.¹⁶ At the 1- q to 3- q transition “islands” of the 3- q phase appear first in the “sea” of the 1- q phase and then gradually take all of the crystal volume. The gradual change of the 1- q NQR line shape (f_{1-q}) to the 3- q NQR line shape (f_{3-q}) is an indication that proustite may exhibit a similar process.

Similar to the 1- q line shape of the high-temperature part of the IC phase, the 3- q line shape of the low-temperature phase remains notably asymmetric. Comparing the experimental spectrum taken at $T=55$ K (Fig. 4) and the theoretical spectrum, calculated in the linear and local approximation [Fig. 1(c)], one can see that one must include more than just the first term in the expansion

$$\begin{aligned} \nu_{3-q}(\varphi_1, \varphi_2, \varphi_3) = & \nu_0 + \nu_1 \sum_{i=1}^3 \cos(\varphi_i + \varphi_{10}) \\ & + \nu_{21} \sum_{i=1}^3 \cos(2\varphi_i + \varphi_{20}) \\ & + \nu_{22} \sum_{i=1}^3 \cos(\varphi_i - \varphi_{i+1}) \\ & + \nu_{23} \sum_{i=1}^3 \cos(\varphi_i + \varphi_j + \varphi_{30}) + \dots \end{aligned} \quad (21a)$$

The line shape is now given by

$$\begin{aligned} f_{3-q}(\nu) = & \int \int \int dx_1 dx_2 dx_3 \\ & \times \delta[\nu - \nu_{3-q}(\varphi_1(\mathbf{r}), \varphi_2(\mathbf{r}), \varphi_3(\mathbf{r}))], \end{aligned} \quad (21b)$$

To describe the gradual change from the 1- q to the 3- q line shape the following fitting procedure was used. First, the spectra in the temperature range 58.5–60 K, where the pure 1- q line shape prevails, were fitted with expression (20). With φ_{10} fixed to zero it was found that the phase shift of the $\cos(2\varphi)$ term φ_{20} does not show any marked temperature dependence, so its value was fixed at the average value $\varphi_{20}(1-q) = 80^\circ$ and the fitting routine was applied again. From this set of fits, the temperature dependence of the parameters ν_1 and ν_2 was determined. As shown in Fig. 5, ν_1 and ν_2 follow a power law $\nu_1 \propto (T_I - T)^{\beta_{1q}}$, $\nu_2 \propto (T_I - T)^{\bar{\beta}_{1q}}$ with $\beta_{1q} = 0.30 \pm 0.02$, $\bar{\beta}_{1q} \approx 2\beta_{1q} = 0.60 \pm 0.02$. Next, the

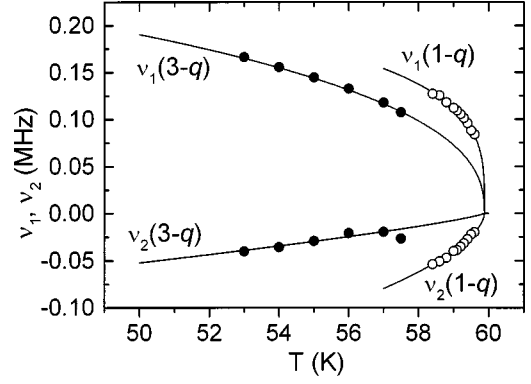


FIG. 5. Temperature dependence of the parameters ν_1 and ν_2 in the 1- q and 3- q phases in proustite. The solid lines are fits to the power law as explained in the text.

spectra in the temperature range 52–57 K, where the 3- q line shape is dominant, were fitted with expression (21). It turned out that “mixed” terms $\cos(\varphi_i - \varphi_{i+1})$ and $\cos(\varphi_i + \varphi_j + \varphi_{30})$ did not improve the quality of the fit, so ν_{22} and ν_{23} were set to zero. Repeated fits with a temperature independent $\varphi_{20}(3-q) = 50^\circ$ yielded the temperature dependence of ν_1 and ν_{21} , shown in Fig. 5. Again a power law with $\beta_{3q} = 0.40 \pm 0.02$ and $\bar{\beta}_{3q} \approx 2\beta_{3q} = 0.81 \pm 0.04$ was obtained. With a known temperature dependence of all the parameters that determine the line shape in both 1- q and 3- q phases the only parameter left to determine is the relative volume fraction of the 1- q phase, $R_{1-q} = V_{1-q}/(V_{1-q} + V_{3-q})$. The intensity of the NQR spectrum in a given frequency interval is proportional to the number of nuclei with the resonance frequency in this interval. If a part of the crystal exhibits a 1- q phase with a frequency distribution $f_{1-q}(\nu)$, and the rest a 3- q phase with frequency distribution $f_{3-q}(\nu)$, the measured line shape will be

$$f(\nu) = R_{1-q} \frac{f_{1-q}(\nu)}{\int f_{1-q}(\nu') d\nu'} + (1 - R_{1-q}) \frac{f_{3-q}(\nu)}{\int f_{3-q}(\nu') d\nu'}. \quad (22)$$

Using this formula, the temperature dependence of “1- q phase fraction” R_{1-q} , shown in Fig. 6, was determined.

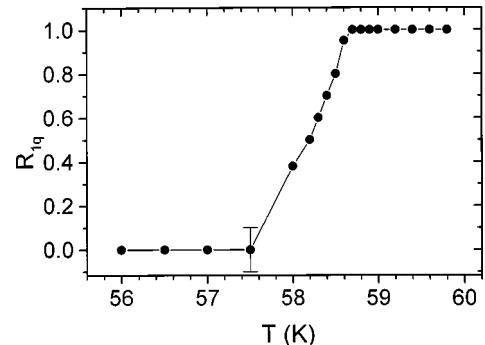


FIG. 6. Temperature dependence of the relative volume fraction of the 1- q stripe phase R_{1-q} at the 1- q to 3- q phase transition. Lines connecting points are a guide to the eye only.

The fact that $R_{1-q} \sim 1$ above 58.5 K and $R_{1-q} \sim 0$ below 57.5 K gives us some confidence in our initial (“pure 1- q ” and “pure 3- q ”) fits.

As pointed out by Ryan *et al.*,¹¹ the ordering of the structure in this temperature range is subject to rather long equilibrium times (several hours or more). It is also known³⁴ that the temperatures of the phase transitions T_I , T_L , and T_{C_2} in proustite depend on cooling or heating rate of the crystal. Our measurements were performed on cooling with a small temperature step ($\Delta T = 0.1\text{--}0.5$ K) and 1 h of temperature stabilization prior to the measurement. Depending on the linewidth, measurement took from half an hour up to several hours in the low-temperature part of the IC phase. Obviously, different cooling rates will produce temperature dependences of $R_{1-q}(T)$, which will be different from that presented in Fig. 5.

The critical behavior at the normal to the incommensurate phase transition for one dimensionally (1- q) modulated IC systems with a two-component order parameter belongs to the two-component three-dimensional XY ($d=3$, $D=2$) universality class.³⁵ The theoretically predicted value $\beta = 0.345$ for the critical exponent of the order-parameter amplitude agrees very well with the β determined from both the NQR and the quadrupole perturbed NMR measurements on several such systems.^{3,30} The critical exponents $\beta_{1q} = 0.3$ and $\beta_{3q} = 0.4$ that we obtained in proustite, both differ from the prediction of the 3D XY model.^{35,36} It is interesting that our value obtained in the 3- q phase of proustite, which is described with a six-component order parameter, agrees very well with the prediction of the six component three-dimensional ($d=3$, $D=6$) Heisenberg model, $\beta = 0.399$.³⁶ In spite of the fact that the relevance of this result must be seriously questioned due to the very long equilibrium times of the structure stabilization and the vicinity of the 1- q to 3- q transition, proustite seems to represent a good candidate for subsequent studies of critical behavior of systems with a six-component order parameter.

D. Variation of T_1 over the NQR spectrum

The striking feature of the spin-lattice relaxation in 1- q IC systems is that T_1 varies over the incommensurably broadened line in such a way that it is possible to separate phason and amplitudon contribution^{3,4,33} to the relaxation rate. In an often realized case, T_1 is determined by the amplitudon fluctuations at the edge singularities, while it is determined by the more effective phason fluctuations in the middle of the spectrum. The measurement of variation of T_1 over the NQR line at $T = 59.5$ K in the 1- q stripe phase of proustite (Fig. 7) shows exactly such a behavior.

In contrast to this, a distribution [Eq. (19)] of relaxation rates T_1^{-1} , determined by the three amplitudon and phason branches [Eq. (18)] is expected in the 3- q case. The short relaxation time $T_1 \sim 200 \mu\text{s}$ and the extremely broad spectrum do not allow us to extract the distribution of relaxation times from the magnetization recovery curves, which seem to be monoexponential within the experimental precision. The average T_1 , which was determined at $T = 58.5$ K in the 3- q phase, does not show any line-shape dependence. While we were not able to extract the characteristic distribution [Eq. (19)] of the relaxation rates, expected for the 3- q IC

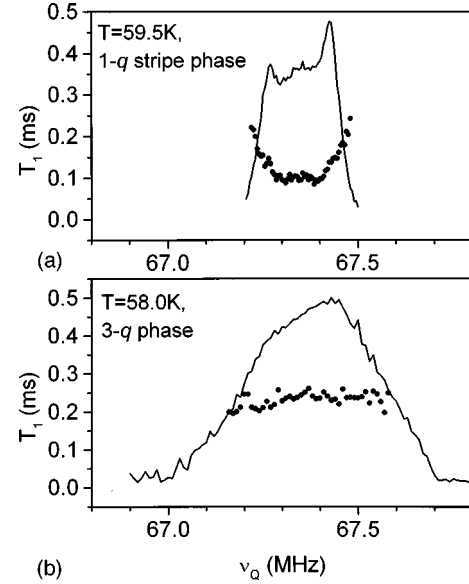


FIG. 7. The variation of the spin-lattice relaxation time T_1 (●) over the NQR line (full line) (a) in the 1- q stripe and (b) in the 3- q nonplanar IC phase in proustite.

phase,¹⁹ the observed change of the variation of T_1 over the NQR line may be taken as an additional evidence for the transition from the 1- q stripe to the 3- q phase in proustite.

E. Line-shape analysis in the low temperature part of the IC phase

Figure 8 shows the ⁷⁵As NQR spectra in the low-temperature part of the incommensurate phase in proustite. Below $T = 52$ K the 3- q line shape begins to show an additional structure. At $T = 50$ K the shoulders of the bell-like spectrum become so pronounced that a valley forms in-between, and an additional structure appears in the high-frequency part of the spectrum. At still lower temperatures narrow peaks begin to gradually rise from the broad 3- q lines. On cooling these peaks increase in intensity and decrease in width and finally completely replace the broad 3- q line shape below $T = 48.5$ K.

A similar type of behavior is often found close to the lock-in transition in 1- q incommensurate systems indicating that the phase of the modulation wave becomes a nonlinear function of the space coordinate, i.e., that a multisoliton lattice is formed.

To check on the nature of the low-temperature part of the 3- q IC phase in proustite one can simplify the Pokrovsky free energy¹⁵ by keeping only the simplest ($D_1 \Sigma_i \eta_i^6$) of the six allowed “lock-in” terms. By minimization of the free energy using Euler-Lagrange equations one obtains $\varphi(u_1)$ as a solution of the ordinary sine-Gordon equation

$$[2(\alpha^2 + \beta^2)\sin^2 \theta + 2(\alpha^2 + \gamma^2)\cos^2 \theta + \epsilon \sin \theta \cos \theta] \varphi''(u_1) = -t^2 D_1 \sin(6\varphi(u_1)). \quad (23)$$

The coefficients α , β , γ , ϵ , and D_1 are defined in Ref. 15 and solutions for φ_2 and φ_3 are equivalent due to the C_3 symmetry.^{11,15} This simplification of Pokrovsky¹⁵ theory, which takes into account only the most simple of the allowed

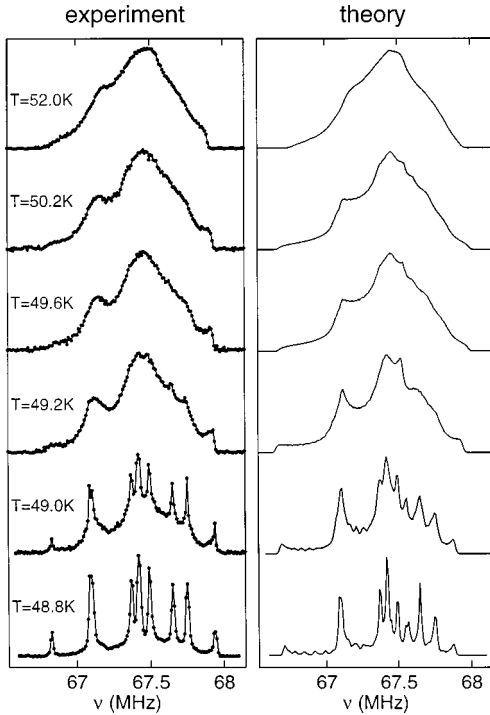


FIG. 8. Experimental and theoretical ^{75}As NQR line shapes in the low-temperature part of the 3- q incommensurate phase in proustite where the phases of the three modulation waves become nonlinear functions of the space coordinates. The temperature dependence of n_s obtained from the theoretical spectra is shown in Fig. 9.

“lock-in” terms D_i therefore predicts that the phases of the modulation waves in the low-temperature part of the 3- q phase in proustite are expressed as solutions of the ordinary sine-Gordon equation, in complete analogy with the well-known examples of one dimensionally modulated incommensurate systems.¹⁻⁴ Of course, the above prediction is just one of the possible scenarios as higher-order terms and interactions between solitons, which we neglected, may considerably influence the result. Nevertheless, it clearly shows that it is quite likely that the phases of the three modulation waves become nonlinear functions of the coordinates, or equivalently, that higher harmonics of the modulation waves develop at lower temperatures. If this is the case, the phase transition to the commensurate phase in proustite is similar to the lock-in phase transition of usual 1- q systems.

Within the above approximation the phases of the modulation waves are independent also in the soliton limit and are given as the elliptic amplitude solutions of the sine-Gordon Eq. (23), $\varphi_1(\mathbf{r}) = \varphi(u_1)$, $\varphi_2(\mathbf{r}) = \varphi(u_2)$ in $\varphi_3(\mathbf{r}) = \varphi(u_3)$,

$$\varphi(u_i) = \frac{2}{p} \text{am} \left(v \frac{p}{2} u_i, k^2 \right). \quad (24)$$

The parameter k is here connected to the linear soliton density,³ $n_s = \pi / (2K(k))$, $K(k)$ is the complete elliptic integral of the first kind, u_i are the space coordinates in the directions of the modulation wave vectors \mathbf{q}_i , while the parameter p is connected with the unit-cell multiplication. In the preset case we have $p=6$ for the transition to C_1 phase with the tripling of the edge of the unit cell. In the plane-wave limit where φ is a linear function we have $k=0$ and

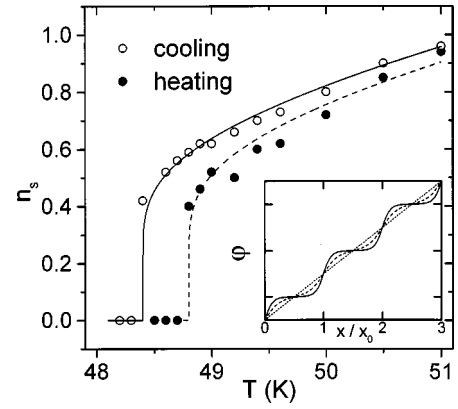


FIG. 9. Temperature dependence of the soliton density n_s in proustite. The inset shows the phase of incommensurate wave for $n_s=1$ (straight dotted line), $n_s=0.5$ (dashed line), and $n_s=0.25$ (full line).

$n_s=1$. On cooling n_s decreases and φ becomes more and more steplike (see inset to Fig. 9). In 1- q incommensurate systems the soliton density n_s represents the domain-wall (soliton) volume fraction of the crystal, $n_s = d_0/x_0$. Here d_0 is the soliton width and x_0 is the distance between the solitons.³ In the 3- q case this meaning is lost and one must regard n_s as a parameter that describes the nonlinearity of the phases of modulation waves.

In our approximation the NQR line shape is again evaluated with the integral (21b), but the phases of the modulation waves are no longer linear functions and are given by Eq. (24). The parameter k , which determines n_s , was chosen to give the best fit to the experimental data. The narrow (“commensurate” or C) lines, which rise from the broad background at lower temperatures, originate from regions where the phase φ is almost constant. The value of the initial phase φ_{10} in the $v_1 \sum \cos(\varphi_i + \varphi_{10})$ term of Eq. (21), which influences the positions of these lines in the multisoliton limit (but does not affect the line shape in the plane-wave limit) was chosen to give the best agreement between the experimental and the calculated line positions. As shown in Fig. 8, the theoretical and the experimental spectra agree rather well. The fact that the positions of every C line could not be reproduced completely is an indication that more than two terms in the expansion (21a) should be taken into account or that the constant amplitude approximation is not strictly valid in this temperature range.

The temperature dependence of n_s , obtained from both cooling and heating experiments, is shown in Fig. 9. The transition to C_1 is reached when n_s vanishes. A hysteresis of 0.6 K at the IC-C transition agrees well with the x-ray measurements by Ryan *et al.*¹¹

Phenomenologically one can treat the IC-C transition by writing the free-energy density in the narrow soliton limit^{14,15,37}

$$f \sim \varepsilon_s n_s + \varepsilon_2 n_s^2 + \varepsilon_3 n_s^3 + a_2 n_s \exp(-n_s^{-1}). \quad (25)$$

The first term represents the energy of a domain-wall (soliton), $\varepsilon_s \propto (T_L - T)$, ε_2 and ε_3 are the energies of double and triple domain-wall crossings, and the last term represents the interaction between the domain walls.³⁷ If the 3- q phase is

TABLE I. In the C_1 phase the phases of the three modulation waves φ_i take commensurate values ϑ_1 , ϑ_2 , and ϑ_3 . The intensities of the ten resonant lines in the NQR spectrum are proportional to the number of permutations of phases ϑ_i , corresponding to a given frequency.

Index	φ_1	φ_2	φ_3	Number of permutations =line intensity
1	ϑ_1	ϑ_1	ϑ_1	1
2	ϑ_2	ϑ_2	ϑ_2	1
3	ϑ_3	ϑ_3	ϑ_3	1
4	ϑ_1	ϑ_2	ϑ_2	3
5	ϑ_1	ϑ_3	ϑ_3	3
6	ϑ_2	ϑ_1	ϑ_1	3
7	ϑ_2	ϑ_3	ϑ_3	3
8	ϑ_3	ϑ_2	ϑ_2	3
9	ϑ_3	ϑ_1	ϑ_1	3
10	ϑ_1	ϑ_2	ϑ_3	6
Σ	10 peaks			$Z_{C_1}=27*Z_N$

preferred over the $1-q$ phase, then ε_3 must be negative and an IC-C transition is necessarily discontinuous. Still, within the precision of our experiment, the temperature dependence of n_s in proustite (Fig. 9) is well described by $n_s \propto -1/\ln[(T-T_L)/T_L]$, which is characteristic of an almost continuous ‘‘lock-in’’ transition as seen in some $1-q$ systems.³

Below the IC- C_1 transition n_s is zero and the incommensurate frequency distribution is replaced by a multiplet of narrow lines reflecting the multiplication of the unit cell. Here the phases of the three modulation waves φ_i become step functions, taking the commensurate values $\vartheta_1=\pi/3$, $\vartheta_2=\pi$, and $\vartheta_3=5\pi/3$ only. For every combination of com-

mensurate values of phases $\varphi_1(\mathbf{r})=\vartheta_i$, $\varphi_2(\mathbf{r})=\vartheta_j$, $\varphi_3(\mathbf{r})=\vartheta_k$, there is a corresponding peak in the NQR spectrum at the frequency $\nu_{3-q}(\vartheta_i, \vartheta_j, \vartheta_k)$ [see Eq. (21)]. The narrow resonance line from the high-temperature N phase should therefore split into $n=3^3=27$ lines, but many lines in the C_1 phase overlap, since ν_{3q} is invariant to the permutation of the phases ϑ_i , ϑ_j , and ϑ_k (see Table I). As predicted in Table I, the NQR spectrum in the C_1 phase consists of three lines with relative intensity 1, six lines with relative intensity three, and a single line with the relative intensity 6. This agrees well with the spectrum in the C_1 phase at 28 K (Fig. 3).

VI. CONCLUSIONS

In conclusion, our ⁷⁵As NQR line-shape and spin-lattice relaxation time measurements have shown that proustite exhibits not one, but two incommensurate phases in the temperature range 49–60 K. As demonstrated by the characteristic NQR line-shape and spin-lattice relaxation time dependence over the line, the phase 58.5–60 K is a $1-q$ stripe phase, where the amplitude of only one of the three possible incommensurate modulation waves is different from zero in a given domain. Below 58.5 K a new $3-q$ phase gradually appears. The stripe phase disappears below 57.5 K. In the $3-q$ phase the amplitudes of all modulation waves are different from zero simultaneously. The NQR line shape shows that the three modulations are noncoplanar and therefore independent.

In the low-temperature part of the $3-q$ IC phase the phases of modulation waves become nonlinear functions of the space coordinates and a multisoliton lattice is formed. By comparison of the theoretical and the experimental spectra, a temperature dependence of the soliton density at the transition to the commensurate phase was determined.

¹P. Bak and J. V. Emery, Phys. Rev. Lett. **36**, 978 (1976).

²W. L. McMillan, Phys. Rev. B **14**, 1496 (1976).

³*Incommensurate Phases in Dielectrics*, edited by R. Blinc and A. P. Levanyuk (North-Holland, Amsterdam, 1986), Vol. I.

⁴R. Blinc, Phys. Rep. **79**, 331 (1981).

⁵B. H. Suits, S. Couturie, and C. P. Slichter, Phys. Rev. Lett. **45**, 194 (1980).

⁶D. E. Moncton, J. D. Axe, and F. J. DiSalvo, Phys. Rev. B **16**, 801 (1977).

⁷C. H. Chen, J. M. Gibson, and R. M. Fleming, Phys. Rev. Lett. **47**, 723 (1981).

⁸For a review, see G. Dolino, in *Incommensurate Phases in Dielectrics* (Ref. 3), Vol. I, p. 205.

⁹T. Apih, U. Mikac, A. V. Kityk, and R. Blinc, Phys. Rev. B **55**, 2693 (1997).

¹⁰P. Saint Gregoire, I. Luk'yanchuk, Ferroelectrics **191**, 267 (1991); M. Vallade, V. Dvorak, and J. Lajzerovitz, J. Phys. (Paris) **48**, 1171 (1987).

¹¹T. W. Ryan, A. Gibaud, and R. J. Nelmes, J. Phys. C **18**, 5279 (1985).

¹²S. S. Khasanov and V. Sh. Shekhman, Ferroelectrics **67**, 55 (1986).

¹³A. V. Bondar, V. S. Vikhnin, S. M. Ryabchenko, and V. E.

Yachmenev, Fiz. Tverd. Tela (Leningrad) **25**, 2602 (1983) [Sov. Phys. Solid State **25**, 1497 (1983)].

¹⁴J.-C. Tolédano and P. Tolédano, *The Landau Theory of Phase Transitions* (World Scientific, Singapore, 1987).

¹⁵V. L. Pokrovsky and L. P. Pryadko, Fiz. Tverd. Tela (Leningrad) **29**, 1492 (1987) [Sov. Phys. Solid State **29**, 853 (1987)].

¹⁶K. Parlinski and G. Chapuis, Phys. Rev. B **47**, 13 983 (1993); **49**, 11 643 (1994).

¹⁷S. V. Dmitriev, T. Shigenari, and K. Abe, Phys. Rev. B **58**, 2513 (1998).

¹⁸A. D. Bruce and R. A. Cowley, J. Phys. C **11**, 3609 (1978).

¹⁹R. Blinc and S. Žumer, Phys. Rev. B **41**, 11 314 (1990).

²⁰T. Apih, U. Mikac, J. Seliger, J. Dolinšek, and R. Blinc, Phys. Rev. Lett. **80**, 2225 (1998).

²¹D. Harker, J. Chem. Phys. **4**, 381 (1936).

²²D. Baisa, A. Bondar, A. Gordon, and S. Maltsev, Phys. Status Solidi B **93**, 805 (1979).

²³S. R. Yang and K. N. R. Taylor, Phase Transit. **36**, 233 (1991).

²⁴P. J. S. Ewen, W. Taylor, and G. L. Paul, J. Phys. C **16**, 6475 (1983).

²⁵R. J. Nelmes, C. J. Howard, T. W. Ryan, W. I. F. David, A. J. Schultz, and P. C. W. Leung, J. Phys. C **17**, L861 (1984).

²⁶S. Allen, Phase Transit. **6**, 1 (1985).

- ²⁷R. Blinc, J. Seliger, and S. Žumer, J. Phys. C **18**, 2313 (1985).
- ²⁸J. M. Perez-Mato, R. Walisch, and J. Petersson, Phys. Rev. B **35**, 6529 (1987).
- ²⁹J. D. Axe, M. Izumi, and G. Shirane, in *Incommensurate Phases in Dielectrics* (Ref. 3), Vol. II, p. 1.
- ³⁰R. Walisch, J. M. Perez-Mato, and J. Petersson, Phys. Rev. B **40**, 10 747 (1989).
- ³¹C. Meinel, H. Zimmermann, and U. Haeberlen, Phys. Rev. B **56**, 13 774 (1997).
- ³²J. A. Norcross and D. C. Ailion, Solid State Commun. **98**, 119 (1996).
- ³³S. Žumer and R. Blinc, J. Phys. C **14**, 465 (1981).
- ³⁴I. M. Shmytko, N. S. Afonikova, and N. A. Dorkhova, Fiz. Tverd. Tela (St. Petersburg) **40**, 2217 (1998) [Phys. Solid State **40**, 2013 (1998)].
- ³⁵R. A. Cowley and A. D. Bruce, J. Phys. C **11**, 3577 (1978).
- ³⁶K. G. Wilson and J. Kogut, Phys. Rep. **12**, 75 (1974).
- ³⁷P. Bak, D. Mukamel, J. Villain, and K. Wentowska, Phys. Rev. B **19**, 1610 (1979).